ACS Infectious Diseases

pubs.acs.org/journal/aidcbc

Letter

Selectively Targeting and Differentiating Vancomycin-Resistant *Staphylococcus aureus via* Dual Synthetic Fluorescent Probes

Tsung-Shing Andrew Wang,* Pin-Lung Chen, Yi-Chen Sarah Chen, Hsuan-Min Hung, and Jhih-Yi Huang

Cite This: https://doi.org/10.1021/acsinfecdis.1c00235

Read Online

ABSTRACT: Many *Staphylococcus* bacteria are pathogenic and harmful to humans. Noticeably, some *Staphylococcus*, including vancomycin-resistant *S. aureus* (VRSA), have become notoriously resistant to antibiotics and have spread rapidly, becoming threats to public health. Here, we designed a dual fluorescent probe scheme combining siderophores and antibiotics as the guiding units to selectively target VRSA and vancomycin-sensitive *S. aureus* (VSSA) in complex bacterial samples. Siderophore-mediated iron uptake is the key pathway by which *S. aureus* acquires iron in limited environments. Therefore, the siderophore-derivative probe could differentiate between *S. aureus* and other bacteria. Moreover, by fine-tuning the vancomycin-derivative probes, we could selectively target only VSSA, further differentiating VRSA and VSSA. Finally, by combining the siderophore-derivative probe and the vancomycin-derivative probe, we successfully targeted and differentiated between VRSA and VSSA in complicated bacterial mixtures.

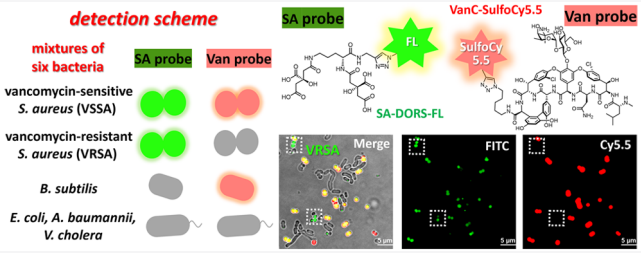

KEYWORDS: *Staphyloferrin A, Staphylococcus bacteria, selective bacterial targeting, siderophore, click chemistry, VRSA*

The discovery and clinical introduction of antibiotics was a key milestone in modern medicine and global public health.[1] Without proper administration of antibiotics, patients might suffer from deadly infections by pathogenic bacteria. However, the rapid and inevitable emergence of antibiotic resistance has rendered antibiotics ineffective.[2] As a result, finding new antibiotics is an urgent priority. Moreover, developing smart diagnostic tools for preventing the misuse and overuse of antibiotics might slow the spread of antibiotic resistance.[3]

In 2017, the World Health Organization (WHO) reported a list of antibiotic-resistant priority pathogens critical to human health, including mostly Gram-negative and two Gram-positive bacteria, which are resistant to β-lactams (e.g., carbapenem, cephalosporin, or methicillin), fluoroquinolones, or vancomycin (**Van**, **1**) (Figure 1b), to call for the research and development of new antibiotics.[4] Among these resistant bacteria, vancomycin-resistant *E. faecium* (VRE) and antibiotic-resistant *S. aureus* are two major Gram-positive bacteria. More strikingly, *S. aureus* was the only bacterium on this list possessing multiple resistance.[4] Although *S. aureus* is a common commensal microbe and opportunistic pathogen, its variants, including methicillin-resistant *S. aureus* (MRSA), cause serious threats to human health due to their notorious resistance against common β-lactams and need to be treated by the "last-resort" **Van**. Hence, this situation is especially worrisome, as infections caused by **Van**-intermediate *S. aureus* (VISA) and **Van**-resistant *S. aureus* (VRSA) have emerged in recent years and become more prominent.[5−7]

Vancomycin kills Gram-positive bacteria by binding to the D-alanyl-D-alanine (D-Ala-D-Ala) moiety of the newly born cell wall and its precursor Lipid II.[8] It is believed that VISA resists **Van** by using enhanced physical barriers to decrease its penetration, while VRSA and VRE have gained resistance by swapping D-Ala-D-Ala into D-alanyl-D-lactate (D-Ala-D-Lac).[9,10] Since *S. aureus* is a common strain in all places, differentiation between VRSA and **Van**-sensitive *S. aureus* (VSSA) is indispensable but challenging.[11−13] However, conventional culturing methods are lengthy and laborious.[14] Therefore, we would like to develop a straightforward protocol using dual fluorescent probes to target VRSA.

To distinguish *S. aureus* from other bacteria, such as *Enterococci*, a *Staphylococcus*-specific probe was required. Given that iron is vital for survival, many microorganisms have evolved several diverse pathways for acquiring iron in iron-limited environments, especially in hosts.[15] Among these pathways, siderophore-mediated iron uptake has drawn increasing scientific attention.[16] Siderophore-based probes

Received: April 28, 2021

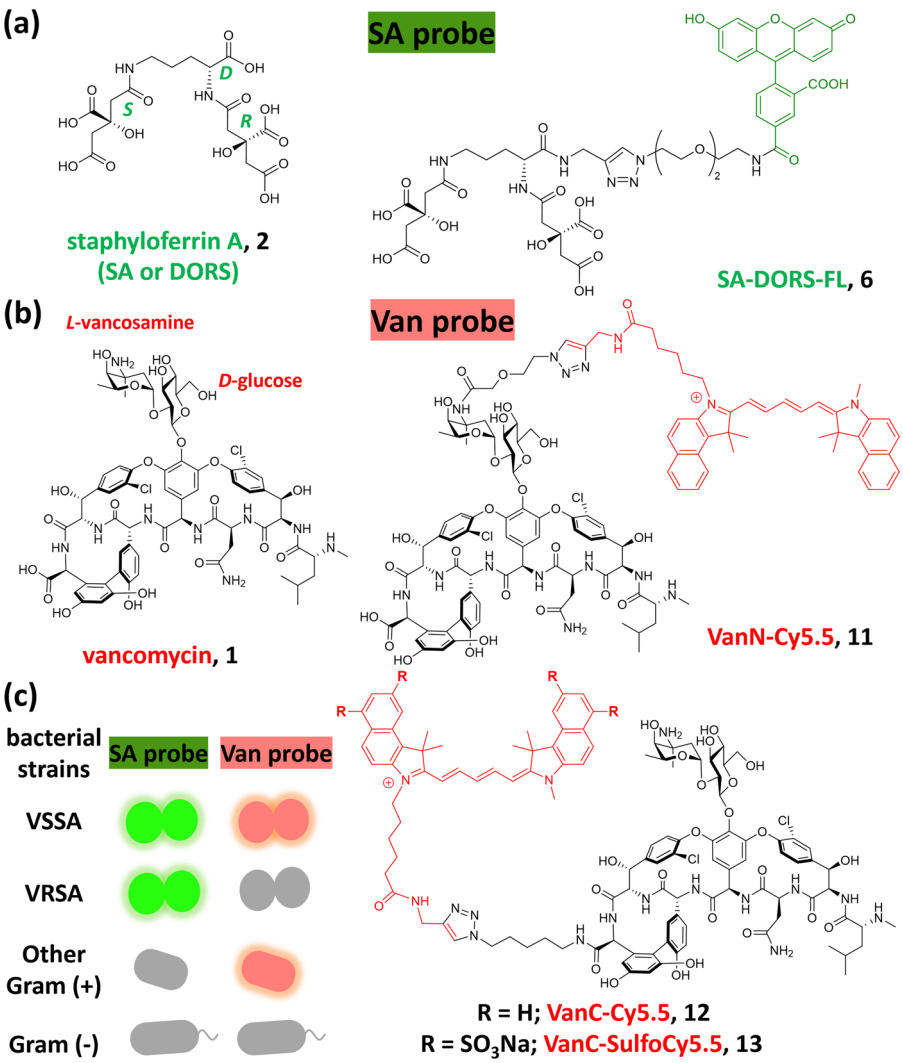

Figure 1. (a) Structures of staphyloferrin A (**SA** or **DORS**, **2**) and its derivatized probe, **SA-DORS-FL** (**6**). (b) Structures of vancomycin (**Van**, **1**) and its derivatized probes, **VanN-Cy5.5** (**11**), **VanC-Cy5.5** (**12**), and **VanC-SulfoCy5.5** (**13**). (c) Detection scheme of **SA**- and **Van**-based fluorescent probes. Possible staining outcomes are shown for four types of bacterial strains.

have been proven to be potential bacterial targeting agents. For *S. aureus*, staphyloferrin A (**SA**, **2**) (Figure 1a) and B (**SB**) are the two major siderophores.[17] Although both **SA** and **SB** were produced under iron restriction during host infections, **SB** seemed to be important for pathogenesis.[18] However, compared to **SB**, **SA** has a simpler structure, which makes preparation of functional conjugates easier.[19−21] **SA** is composed of D-ornithine (D-Orn) and two citrates through amide linkages on both amine groups of D-Orn. While the stereochemistry of the two citrates on **SA** is debated, their absolute configurations were determined as (*R*) and (*S*) based on the cocrystal structure of **SA** with its receptor HtsA.[22] The cocrystal structure also revealed that the carboxylate of D-Orn was not involved in iron chelation or HtsA binding, making it a perfect site for attaching functional cargos.[22] Owing to the structural simplicity of **SA**, we aimed to develop *Staphylococcus*-specific fluorescent probes using **SA** as the guiding unit to effectively and selectively target *S. aureus*.

To prepare **SA** conjugates with functional cargos, our synthesis started from D-Orn as a central hub, where two citrates and one clickable linker can attach. Fluorenylmethyloxycarbonyl (Fmoc) and *tert*-butyloxycarbonyl (Boc) groups were used as orthogonal protection to introduce two citrates with defined (*R*) and (*S*) stereochemistry on α- and δ-amino groups. The clickable linker propargylamide was then attached through an amide linkage in the early stage, where it could be attached with diverse functional cargos through click chemistry, such as copper(I)-catalyzed azide alkyne cycloaddition (CuAAC). Finally, we were able to prepare **SA-alkyne**, namely, **DORS-3**, from four building blocks, D-Orn, (*R*)-, (*S*)-citrates (**4**), and propargylamide. Moreover, **DORS-3** and **azFL** (**5**) were linked by CuAAC to afford the fluorescent probe, **SA-DORS-FL** (**6**) (Figure 1a and Scheme S1).

For the detection of **Van** resistance, **Van**-based fluorescent probes have been used to image bacterial cell wall dynamics[23] and label Gram-positive bacteria as diagnostic tools.[24−26] Most of the applications relied on the affinity between **Van** and the cell wall D-Ala-D-Ala residues. Hence, these probes label **Van**-sensitive bacteria. To exclusively report **Van** resistance, our probes need to be optimized to avoid false-positive binding of **Van**-resistant bacteria (Figure 1c). We chose the amino group of vancosamine and the carboxyl terminal of the **Van** aglycone, commonly used to attach various linkers for further functionalization.[27,28] First, 2-(2-chloroethoxy) ethanol was

https://doi.org/10.1021/acsinfecdis.1c00235
ACS Infect. Dis. XXXX, XXX, XXX−XXX

reacted with sodium azide, followed by Jones oxidation to form the corresponding azido carboxylic acid linker. After activation by an *N*-hydroxysuccinimidyl (NHS) ester, the azido linker was attached to **1** through amide bond formation. The resulting **VanN-azide** (**7**) was purified by HPLC (Scheme S2). Second, 1,5-pentadiol was brominated to form 1,5-dibromopentane before being converted into a diazido derivative by reacting with sodium azide. Using the heterogeneous Staudinger reduction, 1,5-diazidopentane was then partially reduced to form the linker 1-azido-5-aminopentane, which was then reacted with **1** in the presence of HBTU to afford **VanC-azide** (**8**) before HPLC purification (Scheme S3). Finally, using CuAAC, **7** and **8** were linked together with commercial **Cy5.5-alkyne** (**9**) or **SulfoCy5.5-alkyne** (**10**) to afford the **Van** probes **VanN-Cy5.5** (**11**), **VanC-Cy5.5** (**12**), and **VanC-Sulfo-Cy5.5** (**13**) (Figure 1b and Scheme S3). (Note: In some CuAAC reactions, the cycloaddition efficiency can be significantly improved by supplementation with tris[(1-(2-ethoxy-2-oxoethyl)-1*H*-1,2,3-triazol-4-yl)methyl]amine (TEOTA) as the Cu(I) stabilizing ligand.)

We noticed that **VanN** derivatives **7** and **11** lost their acylated vancosamine moiety to a certain extent and were particularly notable when trifluoroacetic acid (TFA) was used as an additive in HPLC. In contrast, during the preparation and biological experiments, **VanC** derivatives **8**, **12**, and **13** seemed stable, as the amino group of the vancosamine moiety was intact. In the hydrolysis reaction, the formation of the positive oxocarbenium intermediate on vancosamine is a key step and will facilitate the breakage of the glycosylic bond between vancosamine and glucose. Since the amino group of vancosamine in **Van** can be protonated by TFA to form ammonium ions, this positively charged functional group can prevent the formation of the positive oxocarbenium intermediate and therefore resist hydrolysis. However, when amidated, such as in **VanN** derivatives **7** and **11**, the amino group of vancosamine lost its protonation ability, causing the glycosylic bond between amidated vancosamine and glucose to break more easily (Figure S4).

Using fluorescence microscopy, we showed that **6** specifically targeted *S. aureus* under iron-limiting conditions by adding 200 μM 2,2′-dipyrdine (**DP**). Other bacteria, *E. faecalis*, *B. subtilis*, and *E. coli*, were not targeted (Figure 2). **DP** is frequently used in iron limitation.[19] The attachment of the triazole click linker, PEG linker, and fluorescein did not affect the targeting ability and selectivity of **6**. In addition, 2−10 μM control **5** and probe **6** did not affect bacterial growth during our uptake experiments. Compared to controls without **5** or **6**, the bacterial morphology and quantity did not change when **5** or **6** was added. To confirm the iron dependency of our probe **6**, we compared the labeling by **6** in *S. aureus* under different levels of iron-limitation, ranging from restricted to abundant iron conditions.

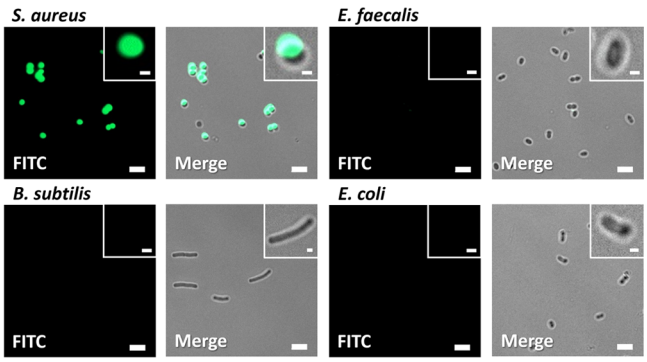

Figure 2. Demonstration of selective bacterial labeling by **SA-DORS-FL** (**6**) using fluorescence microscopy. Bacteria were treated with probe **6** (2.5 μM probe at 37 °C for 4 h) with **DP** (200 μM). Scale bar: 5 μm (full) or 0.5 μm (enlarged).

Clearly, labeling was profound under restricted conditions (200 μM **DP**) and decreased as the amount of supplemented free iron increased (Figure S5). The labeling was still notable in LB with only residual iron (0 μM Fe). When extra iron was supplemented (10−100 μM Fe), the labeling was abolished. The correlation between labeling and iron-limitation showed a strong iron dependency of labeling by **SA-DORS-FL** (**6**), suggesting that our probe targeted *S. aureus* through the siderophore-mediated iron uptake pathway, as shown previously.[20]

Then, with **SA** and **Van** probes in hand, we examined their targeting efficiency and strain selectivity. When using probe **6** in combination with three other **Van** probes under iron-limiting conditions, both VSSA SA113 and the clinical isolate of VRSA NR-49120 could still be efficiently labeled by **6**, while non-*Staphylococcus* bacteria, including *E. faecalis*, *B. subtilis*, and *E. coli*, could not be labeled. Notably, the labeling efficiency of VSSA was better than the labeling efficiency of VRSA, possibly due to the thicker cell walls in VRSA (Figures 3a, S6a and S7a). In contrast, three **Van** probes behaved differently in bacterial labeling. **VanN-Cy5.5** (**11**) only weakly labeled non-**Van**-resistant Gram-positive bacteria, including VSSA, *E. faecalis*, and *B. subtilis*, causing a 10- to 110-fold fluorescence increase (Figure S6b). **VanC-Cy5.5** (**12**) and **VanC-SulfoCy5.5** (**13**) strongly labeled three non-**Van**-resistant Gram-positive bacteria. However, both Cy5.5- containing **11** and **12** also more or less labeled VRSA and VRE. Notably when VRE was treated with **12**, the labeling was very high (Figure S7b). In contrast, **13** only limitedly labeled VRSA and VRE (Figure 3b), despite the non-negligible VRE labeling. In particular, when comparing the labeling between VSSA and VRSA by our three probes, **13** exhibited the highest labeling intensity when targeting VSSA (110-, 500-, and 1000-fold for **8**, **12**, and **13**, respectively) (Figures 3b, S6b, and S7b) and the greatest intensity ratio of VSSA/VRSA (5.7 vs 1.8 and 42 for **11**, **12**, and **13**, respectively) (Figures 3b, S6b, and S7b), making probe **13** a better candidate for our detection protocol development.

Similar to the flow cytometry results, probe **6** labeled VSSA and VRSA exclusively in fluorescence microscopy (Figures 3c, S6c, and S7c), once again showing its unique *Staphylococcus* targeting specificity. Additionally, all three **Van** probes, **11**, **9**, and **13**, successfully labeled VSSA, *E. faecalis*, and *B. subtilis*. Nevertheless, **13** still exhibited the greatest fluorescence intensity of VSSA labeling in the same image settings (Figures 3c, S6c, and S7c). However, probe **12** unexpectedly labeled VRE quite well (Figure S7c).

The observed labeling of some **Van** probes to the D-Ala-D-Lac-dominant VRSA and VRE seemed confusing and contradictory to previous knowledge. After examining the dose-dependent labeling of three **Van** probes, we observed that a high dose (5 μM) might cause cell lysis. In addition, by measuring MICs (Table 1), we noticed that **11** and **12** killed VSSA as expected, but unlike **Van**, they also killed VRSA and even *E. coli* at concentrations as low as 4−8 μM. However, **13** behaved similarly to **Van**, efficiently killing VSSA but not

https://doi.org/10.1021/acsinfecdis.1c00235
ACS Infect. Dis. XXXX, XXX, XXX−XXX

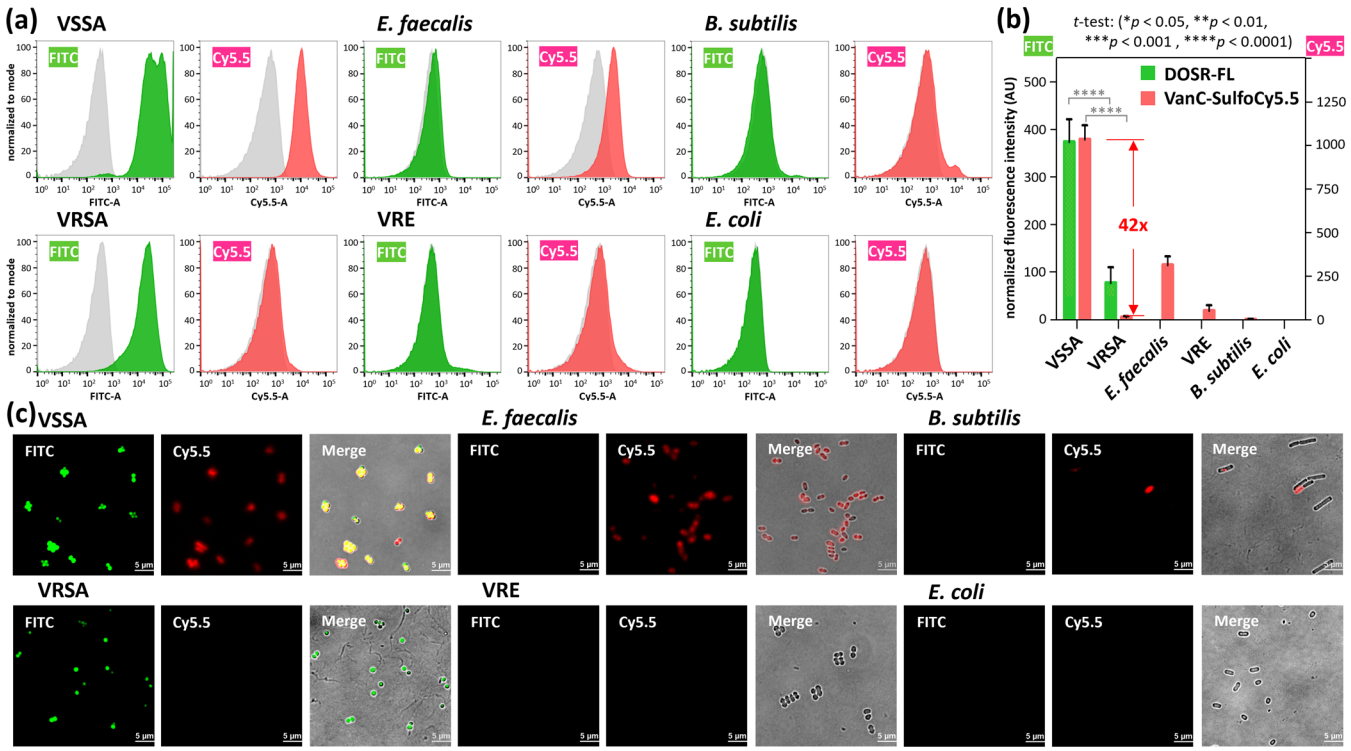

Figure 3. Strain-selectivity of **SA-DORS-FL** (**6**) and **VanC-SulfoCy5.5** (**13**) by flow cytometry and fluorescence microscopy. (a) Flow cytometric histograms of various bacteria treated with 5 μM **6** (green, FTIC channel) and 0.5 μM **13** (red, Cy5.5 channel) under iron-limiting conditions (200 μM **DP** at 37 °C for 4 h). 5 μM **azFL** (**5**) and 0.5 μM **SulfoCy5.5-alkyne** (**10**) were used as the negative controls (gray). (b) Quantification of fluorescence intensity in (a). Bars represent fluorescence intensity normalized against the respective measured negative controls (median ± SD, in triplicate). (c) Fluorescence microscopic images of various bacteria labeled with 5 μM **6** (FTIC channel) and 0.5 μM **13** (Cy5.5 channel) under iron-limiting conditions (200 μM **DP**) (scale bar: 5 μm). Green, red, and yellow colors represent the FTIC, Cy5.5, and FTIC/Cy5.5 (both) channels, respectively.

Table 1. MIC of Bacterial Strains

Compound	MIC (μM)		
	VSSA[a]	VRSA[b]	*E. coli*[c]
1 (vancomycin, **Van**)	1	256	256
9 (**Cy5.5-alkyne**)	2	1	4
10 (**SulfoCy5.5-alkyne**)	32	32	16
11 (**VanN-Cy5.5**)	1	4	4
12 (**VanC-Cy5.5**)	2	8	8
13 (**VanC-SulfoCy5.5**)	4	64	32

[a]VSSA (vancomycin-sensitive *S. aureus*), SA113. [b]VRSA (vancomycin-resistant *S. aureus*), NR-49120. [c]*E. coli* (*Escherichia coli*, CFT073).

VRSA and *E. coli*. As a reference, the MIC of Cy5.5-containing **9** was as low as the MIC of typical antibiotics, while SulfoCy5.5-containing **10** was not considered to be toxic. Hence, we realized that Cy5.5 in **11** and **12** was too toxic to bacteria, possibly due to its hydrophobicity, causing nonspecific binding to the cell membrane as well as false positive fluorescent signals. The hydrophobicity and toxicity should be noteworthy, since Cy5.5 is frequently used in biological probes. SulfoCy5.5 seemed not as toxic as Cy5.5 and is a better fluorophore for biological labeling. However, the multiple negative charges on sulfoCy5.5 could interfere with the binding of the bacterial membrane and reduce nonspecific binding. As a result, SulfoCy5.5-containing derivatives were less toxic than Cy5.5-containing derivatives (Table 1). More impressively, the multiple negative charges on sulfoCy5.5 do not seem to affect the binding of **Van**, as shown in our results and other related reports.[24] Therefore, combined with the fact that the **VanN**-derivatives were not stable, SulfoCy5.5-containing **VanC**-derivative **13** at low concentrations (0.5 μM) was finally chosen for further applications.

Finally, the differentiation protocol between VRSA and VSSA by our dual fluorescent probes **6** and **13** was examined in complex bacterial mixtures. First, either VSSA or VRSA was premixed with four other bacteria, including *B. subtilis*, *E. coli*, *A. baumannii*, and *V. cholerae*, before our dual probe treatment under iron-limiting conditions. As a result, VSSA was labeled as green/red spots (Figure 4a, solid boxes), while VRSA was labeled as green spots in the mixture by fluorescence microscopy (Figure 4a, dashed boxes). Encouraged by the results, mixtures of both VRSA and VSSA, alone and with four other bacteria, were tested by our dual probe protocol. Several VRSA red spots were identified (Figure 4b, dashed boxes), and many VSSA green/red spots were also labeled (Figure 4b) in the selected field of views (FOVs). Rod-shaped *B. subtilis* was targeted as red spots, while other pathogenic Gram-negative bacteria, including *E. coli*, *A. baumannii*, and *V. cholerae*, remained dark as predicted (Figure 1c). These imaging results confirmed that our dual fluorescent probes could efficiently distinguish VRSA from VSSA and other bacteria in the mixtures.

In summary, we developed a VRSA detection scheme that utilized two optimized fluorescent probes **SA-DORS-FL** (**6**) and **VanC-SulfoCy5.5** (**13**). By simultaneously utilizing our two probes in flow cytometry and fluorescence microscopy, VRSA can be labeled in a unique color pattern and

https://doi.org/10.1021/acsinfecdis.1c00235
ACS Infect. Dis. XXXX, XXX, XXX−XXX

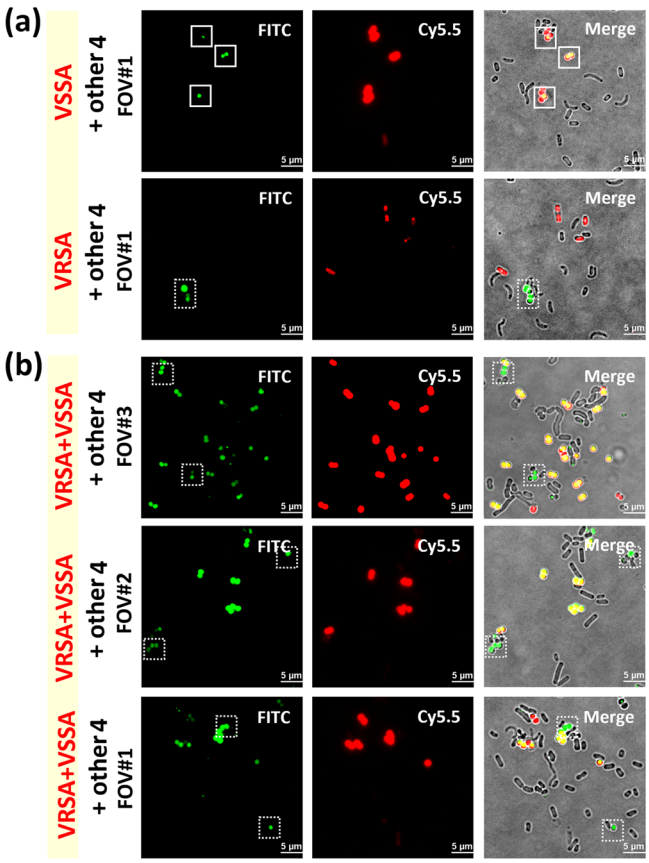

Figure 4. *Staphylococcus*-specific and **Van**-resistant labeling in mixed bacteria samples with the dual probes **SA-DORS-FL** (**6**) and **VanC-SulfoCy5.5** (**13**) using fluorescence microscopy. (a) VSSA (yellow dots, solid box) or VRSA (green dots, dashed box) and (b) both VSSA and VRSA (dashed box) were treated with probes **6** (5 μM) and **13** (0.5 μM) in the presence of four non-*Staphylococcus* bacteria, including *B. subtilis*, *E. coli*, *A. baumannii*, and *V. cholera*, (37 °C for 4 h) with 200 μM **DP**. Green, red, and yellow colors represent the FTIC, Cy5.5, and FTIC/Cy5.5 (both) channels, respectively. FOV: field of view; scale bar: 5 μm.

distinguished from other Gram-positive and Gram-negative bacteria, even from VSSA and other VREs. VISA did not contain D-Ala-D-Ala, and therefore could not be distinguished from VSSA with our detection protocol (data not shown). Probe **6** showed supreme *Staphylococcus* specificity. Since VRSA lacked D-Ala-D-Ala for **Van** binding, probe **13** detected VRSA as a "negative" event. Although we fine-tuned the fluorophores and the linkage site on **Van**, a detection protocol using **SA** and **Van** to "positively" label VRSA and differentiate between VRSA and VSSA might still be desired. Clinical samples might contain many interfering substances that could alter the fluorescence of dual probes. Sample pretreatments, such as subculturing into LB medium or resuspension into PBS buffer, might be preferable prior to our detection protocol in the future medical applications.

■ METHODS

Chemical Synthesis. Compounds were synthesized from commercially available starting materials and fully characterized by nuclear magnetic resonance spectroscopy and mass spectrometry. Full experimental details and analytical data are provided in the Supporting Information.

General Biological Materials and Methods. Several bacterial strains used in this study are listed in Table S1. Brain and heart infusion (BHI) and Luria−Bertani (LB) media were prepared for bacterial cultivation. Media containing 100 μg/mL vancomycin were used for culturing vancomycin-resistant strains. A single colony from the stock agar plate was added to 2 mL of liquid medium with or without vancomycin and then grown at 37 °C in a shaker incubator (200 rpm) overnight followed by subculture until the OD600 value reached 0.5−0.7.

Minimum Inhibitory Concentration (MIC). One day before the experiments, fresh cultures of VSSA SA113, VRSA NR-49120, and *E. coli* CFT073 were inoculated and grown in an orbital shaker at 37 °C in 100% LB. Trace vancomycin was provided, especially in VRSA culture. After 18 h, the bacterial stock solutions were adjusted to a germ solution with an OD600 of 0.5. These diluted bacterial stock solutions were then inoculated into a well of a V-shaped 96-well glass-coated microtiter plate, and supplemented with serially diluted aliquots of the solutions of vancomycin, vancomycin conjugates, and two different dyes in DMSO (4 μL) to achieve a total assay volume of 100 μL. After incubation for 16 h at 37 °C, the MIC values were determined through standard MTT assays. The results are summarized in Table 1.

Flow Cytometry Analysis and Fluorescence Microscopy for SA-DORS-FL Probes. The bacteria (VSSA SA113, *E. faecalis* ATCC 29212, *B. subtilis* ATCC 23857, and *E. coli* CFT073) stored at −80 °C were first revived by incubation in LB media (tryptone 10 g/L, yeast extract 5 g/L, NaCl 10 g/L) for each bacterial strain at 37 °C overnight with shaking at 220 rpm. Then, 100 μL of the overnight bacterial culture was spun down, the supernatant was removed, and the cells were resuspended in minimal iron limiting or rich media (100 μL LB medium supplemented with 200 μM 2,2′-dipyridyl (**DP**) or various concentrations of iron(III) chloride). The spin-down resuspension procedure was repeated three times. The cell density was adjusted to OD600 = 0.5. The **SA-DORS-FL** (**6**) stock solution (1 mM) was added to the bacterial culture to a designated concentration (details in Figures 2 and S5) in 100 μL, and the resulting culture was incubated at 200 rpm and 37 °C for 4 h. Then, 100 μL of bacterial culture was spun down, the supernatant was removed, and the cells were resuspended in 100 μL of PBS (NaCl 8 g/L, KCl 0.2 g/L, Na_2HPO_4 1.44 g/L, KH_2PO_4 0.24 g/L). The spin-down resuspension procedure was repeated three times. 1 μL of bacterial solution was then loaded onto a microscope imaging slide and covered with a coverslip. The imaging was performed on Axio Observer Z1 (Zeiss) with 63× oil immersion lens. The fluorescent images were monitored by using an FITC channel (excitation 470 nm, emission 518 nm).

Flow Cytometry Analysis and Fluorescence Microscopy for SA-DORS-FL/Van Probes. VSSA SA113, VRSA NR-49120, *E. faecalis* ATCC 29212, VREs, *B. subtilis* ATCC 23857, and *E. coli* CFT073 stocks were inoculated and grown in an orbital shaker at 37 °C in 1 mL BHI (brain and heart infusion) medium, respectively. Additionally, VRSA and VREs were supplied with vancomycin (100 mg/mL, 1000-fold dilution) to induce their expression of Van A operon to resist vancomycin. Then, 100 μL of the overnight bacteria culture was spun down, the supernatant was removed, and the cells were resuspended in 100 μL LB medium with 200 μM bipyridine (**DP**). The spin-down resuspend procedure was repeated 3 times and then adjusted to OD600 = 0.5. **SA-DORS-FL** (**6**) stock solution was added to the bacterial

https://doi.org/10.1021/acsinfecdis.1c00235
ACS Infect. Dis. XXXX, XXX, XXX−XXX

culture to a final concentration of 5 μM and **Van** probe (**VanN-Cy5.5** (**11**), **VanC-Cy5.5** (**12**), or **VanC-SulfoCy5.5** (**13**)) stock was also added to the bacterial solution to a final concentration of 0.5 μM. Pure bacteria served as the control group. Then, the culture was incubated at 200 rpm and 37 °C for 2 h. Then, 100 μL of the bacterial culture was spun down, the supernatant was removed, and the cells were resuspended in 1 mL PBS. The spin-down resuspend procedure was repeated 3 times. Next, 2 μL of the bacterial solution was loaded onto an agarose gel on top of an imaging glass slide and covered with a coverslip. Imaging was performed on Nikon Ti2 inverted microscopy with 100× oil immersion lens. The fluorescein signal was monitored by using the FITC channel (λ_{ex} = 470/λ_{em} = 518 nm) and the NIR fluorophore signals were observed with the Cy5.5 channel (λ_{ex} = 650/λ_{em} = 750 nm) After that, a fraction of 50 μL bacterial solution was diluted 10-fold in PBS for further applications in flow cytometry analysis on a BD Canto II flow cytometer, using 488 nm excitation, 585/42A filter set, and/or 633 nm excitation, APC 660/20 filter set.

Flow Cytometry Analysis and Fluorescence Microscopy for Mixed Samples. VSSA SA113, VRSA NR-49120, *V. cholerae* NCTC 8021, *B. subtilis* ATCC 23857, *A. baumannii* ATCC 19606, and *E. coli* CFT073 stocks were inoculated and grown in an orbital shaker at 37 °C in 1 mL BHI (brain and heart infusion) medium, respectively, and VRSA was additionally supplied with vancomycin (100 mg/mL, 1000-fold dilution) to induce its expression of Van A operon to resist vancomycin. Then, 100 μL of the overnight bacterial culture was spun down, the supernatant was removed, and the cells were resuspended in 100 μL LB medium with 200 μM bipyridine (**DP**). Then, three different combinations of mixtures were divided into the following three groups; **Group 1**: VSSA, *B. subtilis*, *V. cholerae*, *A. baumannii*, and *E. coli*; **Group 2**: VRSA, *B. subtilis*, *V. cholerae*, *A. baumannii*, and *E. coli*; **Group 3**: all six bacterial cultures. All groups of bacterial complex samples were mixed and adjusted to OD600 = 0.5. **SA-DORS-FL** (**6**) stock solution was added to the bacterial culture to a final concentration of 5 μM, and **VanC-SulfoCy5.5** (**13**) stock solution was also added to the bacterial solution to a final concentration of 0.5 μM. The separate mixture of pure bacteria served as the control group. Then, the mixed sample was incubated at 200 rpm and 37 °C for 2 h. Then, 100 μL of the bacterial culture was spun down, the supernatant was removed, and the cells were resuspended in 1 mL PBS. The spin-down resuspend procedure was repeated 3 times. Next, 2 μL of bacterial solution was loaded onto an agarose gel on top of an imaging glass slide and covered with a coverslip for imaging.

■ ASSOCIATED CONTENT

Supporting Information

The Supporting Information is available free of charge at https://pubs.acs.org/doi/10.1021/acsinfecdis.1c00235.

Synthesis and characterizations (HPLC and HR-MS) of **SA**-derivatives, **Van**-derivatives, and other compounds used; procedure for bacterial labeling assays; and other experimental details (PDF)

■ AUTHOR INFORMATION

Corresponding Author

Tsung-Shing Andrew Wang − *Department of Chemistry, National Taiwan University, Taipei 10617, Taiwan (R.O.C.)*; orcid.org/0000-0002-4690-3438; Email: wangts@ntu.edu.tw

Authors

Pin-Lung Chen − *Department of Chemistry, National Taiwan University, Taipei 10617, Taiwan (R.O.C.)*

Yi-Chen Sarah Chen − *Department of Chemistry, National Taiwan University, Taipei 10617, Taiwan (R.O.C.)*

Hsuan-Min Hung − *Department of Chemistry, National Taiwan University, Taipei 10617, Taiwan (R.O.C.)*

Jhih-Yi Huang − *Department of Chemistry, National Taiwan University, Taipei 10617, Taiwan (R.O.C.)*

Complete contact information is available at: https://pubs.acs.org/10.1021/acsinfecdis.1c00235

Notes

The authors declare no competing financial interest.

■ ACKNOWLEDGMENTS

We would like to thank the Ministry of Science and Technology, Taiwan, (MOST 108-2628-M-002-007-MY3, 107-2633-M- 002-001- and 106-2113-M-002-009-MY2 to T.-S.A.W.) and the Center for Emerging Material and Advanced Devices, National Taiwan University (NTU-ERP-108L880107 and 108L880124) for financial support. We would also thank Jiun-Wei Wu and Ya-Wen Zhang for assisting in the preparation of synthetic intermediates and data processing.

■ REFERENCES

(1) Kapoor, G.; Saigal, S.; Elongavan, A. Action and resistance mechanisms of antibiotics: A guide for clinicians. *J. Anaesthesiol. Clin. Pharmacol.* **2017**, *33*, 300−305.

(2) Martinez, J. L.; Baquero, F.; Andersson, D. I. Predicting antibiotic resistance. *Nat. Rev. Microbiol.* **2007**, *5*, 958−965.

(3) Stone, M. R. L.; Butler, M. S.; Phetsang, W.; Cooper, M. A.; Blaskovich, M. A. T. Fluorescent Antibiotics: New Research Tools to Fight Antibiotic Resistance. *Trends Biotechnol.* **2018**, *36*, 523−536.

(4) Willyard, C. The drug-resistant bacteria that pose the greatest health threats. *Nature* **2017**, *543*, 15.

(5) Diallo, O. O.; Baron, S. A.; Abat, C.; Colson, P.; Chaudet, H.; Rolain, J. M. Antibiotic resistance surveillance systems: A review. *J. Glob. Antimicrob. Resist.* **2020**, *23*, 430−438.

(6) Hasan, R.; Acharjee, M.; Noor, R. Prevalence of vancomycin resistant Staphylococcus aureus (VRSA) in methicillin resistant S. aureus (MRSA) strains isolated from burn wound infections. *Tzu Chi Med. J.* **2016**, *28*, 49−53.

(7) McGuinness, W. A.; Malachowa, N.; DeLeo, F. R. Vancomycin Resistance in Staphylococcus aureus. *Yale J. Biol. Med.* **2017**, *90*, 269−281.

(8) Perkins, H. R. Vancomycin and Related Antibiotics. *Pharmacol. Ther.* **1982**, *16*, 181−197.

(9) Williams, D. H.; Bardsley, B. The Vancomycin Group of Antibiotics and the Fight against Resistant Bacteria. *Angew. Chem., Int. Ed.* **1999**, *38*, 1172−1193.

(10) McComas, C. C.; Crowley, B. M.; Boger, D. L. Partitioning the loss in vancomycin binding affinity for D-Ala-D-Lac into lost H-bond and repulsive lone pair contributions. *J. Am. Chem. Soc.* **2003**, *125*, 9314−9315.

(11) Pereira, P. M.; Filipe, S. R.; Tomasz, A.; Pinho, M. G. Fluorescence ratio imaging microscopy shows decreased access of vancomycin to cell wall synthetic sites in vancomycin-resistant

Staphylococcus aureus. *Antimicrob. Agents Chemother.* **2007**, *51*, 3627−3633.
(12) Yang, C.; Ren, C.; Zhou, J.; Liu, J.; Zhang, Y.; Huang, F.; Ding, D.; Xu, B.; Liu, J. Dual Fluorescent-and Isotopic-Labelled Self-Assembling Vancomycin for in vivo Imaging of Bacterial Infections. *Angew. Chem., Int. Ed.* **2017**, *56*, 2356−2360.
(13) Norouz Dizaji, A.; Ding, D.; Kutsal, T.; Turk, M.; Kong, D.; Piskin, E. In vivo imaging/detection of MRSA bacterial infections in mice using fluorescence labelled polymeric nanoparticles carrying vancomycin as the targeting agent. *J. Biomater. Sci., Polym. Ed.* **2020**, *31*, 293−309.
(14) Reisner, B. S.; Woods, G. L. Times to Detection of Bacteria and Yeasts in BACTEC 9240 Blood Culture Bottles. *J. Clin. Microbiol.* **1999**, *37*, 2024−2026.
(15) Neilands, J. B. Siderophores: Structure and Function of Microbial Iron Transport Compounds. *J. Biol. Chem.* **1995**, *270*, 26723−26726.
(16) Conroy, B. S.; Grigg, J. C.; Kolesnikov, M.; Morales, L. D.; Murphy, M. E. P. Staphylococcus aureus heme and siderophore-iron acquisition pathways. *BioMetals* **2019**, *32*, 409−424.
(17) Hammer, N. D.; Skaar, E. P. Molecular mechanisms of Staphylococcus aureus iron acquisition. *Annu. Rev. Microbiol.* **2011**, *65*, 129−147.
(18) Perry, W. J.; Spraggins, J. M.; Sheldon, J. R.; Grunenwald, C. M.; Heinrichs, D. E.; Cassat, J. E.; Skaar, E. P.; Caprioli, R. M. Staphylococcus aureus exhibits heterogeneous siderophore production within the vertebrate host. *Proc. Natl. Acad. Sci. U. S. A.* **2019**, *116*, 21980−21982.
(19) Madsen, J. L.; Johnstone, T. C.; Nolan, E. M. Chemical Synthesis of Staphyloferrin B Affords Insight into the Molecular Structure, Iron Chelation, and Biological Activity of a Polycarboxylate Siderophore Deployed by the Human Pathogen Staphylococcus aureus. *J. Am. Chem. Soc.* **2015**, *137*, 9117−9127.
(20) Pandey, R. K.; Jarvis, G. G.; Low, P. S. Chemical synthesis of staphyloferrin A and its application for Staphylococcus aureus detection. *Org. Biomol. Chem.* **2014**, *12*, 1707−1710.
(21) Milner, S. J.; Seve, A.; Snelling, A. M.; Thomas, G. H.; Kerr, K. G.; Routledge, A.; Duhme-Klair, A. K. Staphyloferrin A as siderophore-component in fluoroquinolone-based Trojan horse antibiotics. *Org. Biomol. Chem.* **2013**, *11*, 3461−3468.
(22) Grigg, J. C.; Cooper, J. D.; Cheung, J.; Heinrichs, D. E.; Murphy, M. E. The Staphylococcus aureus siderophore receptor HtsA undergoes localized conformational changes to enclose staphyloferrin A in an arginine-rich binding pocket. *J. Biol. Chem.* **2010**, *285*, 11162−11171.
(23) Tiyanont, K.; Doan, T.; Lazarus, M. B.; Fang, X.; Rudner, D. Z.; Walker, S. Imaging peptidoglycan biosynthesis in Bacillus subtilis with fluorescent antibiotics. *Proc. Natl. Acad. Sci. U. S. A.* **2006**, *103*, 11033−11038.
(24) van Oosten, M.; Schafer, T.; Gazendam, J. A.; Ohlsen, K.; Tsompanidou, E.; de Goffau, M. C.; Harmsen, H. J.; Crane, L. M.; Lim, E.; Francis, K. P.; Cheung, L.; Olive, M.; Ntziachristos, V.; van Dijl, J. M.; van Dam, G. M. Real-time in vivo imaging of invasive-and biomaterial-associated bacterial infections using fluorescently labelled vancomycin. *Nat. Commun.* **2013**, *4*, 2584.
(25) Wang, W.; Zhu, Y.; Chen, X. Selective Imaging of Gram-Negative and Gram-Positive Microbiotas in the Mouse Gut. *Biochemistry* **2017**, *56*, 3889−3893.
(26) Park, H. Y.; Zoller, S. D.; Hegde, V.; Sheppard, W.; Burke, Z.; Blumstein, G.; Hamad, C.; Sprague, M.; Hoang, J.; Smith, R.; Romero Pastrana, F.; Czupryna, J.; Miller, L. S.; Lopez-Alvarez, M.; Bispo, M.; van Oosten, M.; van Dijl, J. M.; Francis, K. P.; Bernthal, N. M. Comparison of two fluorescent probes in preclinical non-invasive imaging and image-guided debridement surgery of Staphylococcal biofilm implant infections. *Sci. Rep.* **2021**, *11*, 1622.
(27) Hofmann, C. M.; Anderson, J. M.; Marchant, R. E. Targeted delivery of vancomycin to Staphylococcus epidermidis biofilms using a fibrinogen-derived peptide. *J. Biomed. Mater. Res., Part A* **2012**, *100*, 2517−2525.
(28) Mishra, N. M.; Stolarzewicz, I.; Cannaerts, D.; Schuermans, J.; Lavigne, R.; Looz, Y.; Landuyt, B.; Schoofs, L.; Schols, D.; Paeshuyse, J.; Hickenbotham, P.; Clokie, M.; Luyten, W.; Van der Eycken, E. V.; Briers, Y. Iterative Chemical Engineering of Vancomycin Leads to Novel Vancomycin Analogs With a High in Vitro Therapeutic Index. *Front. Microbiol.* **2018**, *9*, 1175.

https://doi.org/10.1021/acsinfecdis.1c00235
ACS Infect. Dis. XXXX, XXX, XXX−XXX